The Probablistic Random Forest Clinico-Statistical Regression Analysis of MER Signals with STN-DBS and Enhancement of UPDRS

Venkateshwarla Rama Raju

Abstract

In this study, we present classification and regression analysis to predict the UPDRS score and its enhancement after the microelectrode STN signal recording (MER) with DBS surgery (implantation of the microelectrode). We hypothesized that a data informed grouping of features extrapolated from MER signals of STN can envisage restore (by decreasing the tremor) and functioning the motor improvement in Parkinson's disease (PD) patients. A random—forest is used to account for unbalanced datasets and multiple observations per PD subject, and showed that only five features of STN-MER signals are sufficient and account for prognosting UPDRS advancement. This finding suggests that STN signal characteristics are maximum correlated to the extent of improvement motor restoration and motor behavior observed in STN DBS.

Keywords

Microelectrode-recording (MER)
Parkinson's disease (PD) • STN-DBS • Classification and prediction • Random forest

V. Rama Raju (✉)
Department of Computer Science and Engineering, CMR College of Engineering & Technology (UGC Autonomous), Kandlakoya, Medchal Rd, 501401 Hyderabad, India
e-mail: drvrr@cmrcet.org; system@ou.ernet.in; idcoucea@hd1.vsnl.net.in

V. Rama Raju
Jawaharlal Nehru Technological University Hyderabad JNTUH, Hyderabad, India

V. Rama Raju
Nizam's Institute of Medical Sciences, Biomedical, Neurology and Neurosurgery, Hyderabad, India

V. Rama Raju
Biomedical Engineering Department, Osmania University College of Engineering (Autonomous), Hyderabad, OU, India

1 Introduction

1.1 Parkinson's Disease

Parkinson's disease (PD) is a chronic complex progressive neurodegenerative brain disorder that belongs to a larger class of disorders called movement disorders. PD is one of the most common neurologic disorders that elders' experience with "severe health hazard" is a devastating diagnosis affecting circa ~2 of every 1000 (2/1000) older adults [1–8]. The causes are unknown and so far no cure [1, 2] and the search for optimal cure is on for the past 2 centuries since the time it was first described by James Parkinson [18]. In PD, one particular population of brain cells those that produce a chemical messenger termed dopamine become impaired and lost over time. The loss of these brain cells causes circuits (basal ganglia circuits) in the brain to function bizarrely and those uncharacteristic circuits effect in movement problems [1]. Basal ganglion is an important organ of the brain mainly mean for our movement and control. Present healings for PD are meant for alleviating the symptoms rather than the disease's progression (For instance, Levedopa—a chemical building block that converts human body into dopamine. It replaces the dopamine that is lost in Parkinson's. However, there are more side effects with this drug), hence fresh hope lies in new research and findings, such a latest classification and prediction of clinical enhancements with microelectrode STN recording with DBS (MER with STN-DBS) [1]. The early signs of the disease may help us understand the progress of the disease because it is more than just these dopamine cells in the brain; it affect other cells as well that we are learning more and more about every day [2]. Therefore, prediction is one of the most significant factors in the detection of PD features at very early stage (say two decades in advance). In this paper, we present the classification and prediction of clinical and/or diagnostic setup in deep brain stimulation (DBS) by using with the help of electro-neuro-physiological MER recordings of STN signals.

L. Lhotska et al. (eds.), *World Congress on Medical Physics and Biomedical Engineering 2018*,
IFMBE Proceedings 68/3, https://doi.org/10.1007/978-981-10-9023-3_9

The PD is characterized by its four classes of cardinal motor features (or symptoms), namely, tremor, postural instability, bradykinesia and rigidity [1–4]. PD is caused by damage to the central nervous system (CNS) [5]. Symptoms similar to PD have been mentioned as "Kampavata" in ancient Indian Hindi documents [6]. The search for optimal cure is on for the last two hundred years ever since it was first discovered by James Parkinson a way back in 1817 [7]. Since then, the disease has become the pathfinder for other neurodegenerative disorders, starting with the discovery of dopamine (in PD, one particular population of the brain cells that produce a chemical messenger to communicate with other cells) deficiency within the basal ganglia, which led to the development of first effective treatment for a progressive neurodegenerative condition [8]. However, it is possible that PD was present long before this landmark description. A disease known as Kampa Vata consisting of *shaking* (*kampa*) and lack of muscular movement (*vata*), existed in ancient India as long as 4500 years ago [9]. Deep brain stimulation (DBS) of subthalamic-nuclei (STN) is a surgical technique proving better results not only for the detection of PD features—symptoms but also significantly reducing tremors and restoring the motor function highly which was invented by the two neuroscientists, namely Benabid and Delong [10, 11]. Its mechanisms are not fully elucidated quantitatively—objectively, though the technique was clinically established. However, the clinical outcome is determined by many factors. Microelectrode-recordings (MER) of subthalamic-nucleus (STN) intraoperatively for targeting during DBS procedures are most useful for deducing inferences. This is because anatomical structural organization provide some clues as to what might be the function of basal ganglia circuits, the inference of function from anatomical structure is exploratory [12, 13]. So far quantitative work was done MER with STN-DBS but subject specific enhancement was not performed. In this study we attempted to quantify also predict the UPDRS subject specific enhancement. Objective PD scale can provide a more complete picture of the neurophysiological basis for PD.

2 Methods

The process for DBS was a one-stage bilateral stereotactic approach using a combined electrode for both MER and macrostimulation. Up to five micro/macro-electrodes were used in an array with a central, lateral, medial, anterior, and posterior position. Final target location was based on test stimulation (intraoperatively). Bilateral STN-DBS performed in our tertiary-care center NIMS hospital Hyderabad (South India).

2.1 MR Image-Targeting

One of the major problem with the targeting subthalamic nucleus is that it is a small biconvex lens diamond structure almond shaped and not clearly detected on MRI due to lack of contrast between the STN and the surrounding structures [1–18]. The STN can be visualized on MRI but other methods such as Lozano's technique where a position 3 mm lateral to the superolateral border of the red nucleus is targeted have been studied and found to be effective areas for stimulation. As the MRI techniques are not absolutely perfect, use of electrophysiological techniques such as microelectrode recording from the subthalamic nucleus as well as intraoperative stimulation have assisted in clearly demarcating the STN. Microelectrode recording can identify subthalamic neurons by their characteristic bursting pattern and their signals clearly identify the nucleus form the surrounding structures. On table stimulation is studied to ensure that the there is optimal benefit with the least side effects and this is the final test to ensure the correct targeting of the STN. All these techniques are normally used in combination during targeting, albeit, the individual role of each modality is still not known.

2.2 MER Signal Acquisition—Recording

Five electrodes (Medtronic maker) were placed in an array with a central, lateral, medial, posterior, and an anterior position placed 2 mm apart, to delineate the borders of the nucleus. The targeting was performed according to Lozano's technique—2 mm sections are taken parallel to the plane of anterior comissure-posterior commissure line and at the level with maximum volume of red nucleus, STN is targeted at 3 mm lateral to the anterolateral border of red nucleus. The co-ordinates are entered into stereocalc software which gives the co-ordinates of the STN. Another neuro navigation frame-link-software is also used to plot the course of the electrodes and to avoid vessels. The surgery is performed with two burr holes on the two sides based on the co-ordinates. Five channels that are introduced with the central channel representing the MRI target while medial and lateral are placed in the X-axis while anterior and posterior are placed in the Y-axis to cover an area of 5 mm diameter. Intra-operative recording was performed in all 5 channels. For performing microelectrode-signal-recording of STN with DBS, five microelectrodes are slowly passed through the STN and recording is performed from ± 10 mm (10 mm above to 10 mm below) the STN calculated on the MRI. STN is identified. Extracellular MER was performed with Medtronic-micro-electrodes having an input-impedance

of 1.1 ± 0.4 mega-Ohms (MΩ's) which was calculated at 220 Hz. Signals were recorded with biological-amplifiers signal average`s (10,000 times-amplification) of the Medtronic Lead-point system, by employing bootstrapping method. Signals were filtered using analog band pass filters with lower and upper cut-off frequencies between 0.5 and 5 kHz (amplifier bandwidth). The signal was sampled at 10 kHz, by using 12-bit-resolution analogue-to-digital converter (A/DC) card (2^N, $N = 12$ dynamic-range giving 4096 sample values) and then later up-sampled to 20-kHz at off-line. The channel with maximum recording and the earliest recording were recorded on both sides. Intraoperative test stimulation was performed in all channels from the level at the onset of MER recording. Stimulation was done at 1mv, 3mv to assess the improvement in bradykinesia, rigidity and tremor. Appearance of dyskinesias was considered to be associated with accurate targeting. Side effects were assessed at 5mv and 7mv to ensure that the final channel chosen had maximum improvement with least side effects. Correlation was assessed between the aspects of MER and the final channel chosen in 20 PD-subjects (40 sides).

2.3 Microelectrode Signal Processing and Feature—Selection

In MER signal processing, local field potentials(LFP) and multi-unit-activity(MUA) signals were gathered by low pass and high pass filtering techniques at cut-off frequency 200 and 500 Hz. Spike-detection was performed by MUA voltage-thresholding. Spike-related-features were assessed by common spike-train-metrics [14, 15]. To examine the behavior of local neuronal populations, the BUA was extracted from the MUA following the procedure [18]. In the same studies, it was suggested that the rationality between the MUA-BUA signal-envelopes and LFP may reveal coherent-activity of small or large neuronal-populations. From every signal, we extracted 89 features. A list of investigative-features and their corresponding-metaphors is given in Table 1.

2.4 Random—Forests

A professional way to alleviate above-fitting is by imparting —training several uncorrelated trees in an ensemble-learner referred to as random-forest (RF), which can be applied for classification and regression. RF's can handle highly non-linear interactions and they can cope with small observations and large-number of predictors. During training phase, each tree in RF is trained using a different subset of data "bootstrap-aggregation" and features "random-subspace method" randomly-sampled with replacement. The data that are left out during construction of each tree are used for validation purposes (Fig. 1).

As building the forest advances, the system generates an internal unbiased-estimate of the generalization error (OOB error) which is then used to identify most important variables. The final OOB prediction for a given observation is the average score attained over-all-trees(regression) or choosing majority within forest(classification), without trees that included this observation during their training-phase. In this study, we used RFs both for classification and regression. In the former case, we extracted features that heuristically classified "good" and "poor" STN-DBS responders, defined as patients that exhibited an "off"-state UPDRS-enhancement above or below 38% [17].

2.5 Model Training and Corroboration

RFs were trained using subject-wise bootstrapping, intriguing separately into account the left-hemisphere(LH) and right-hemisphere(RH) STN-feature vectors of each subject Fig. 1a. Each RF consisted of 300-trees. For classification, each tree was created by choosing randomly with replacement 7/9 "good" responders and 7/11 "poor" responders. Therefore, the training pool envisaged 14 feature-vectors (7 PD-subjects × 2 hemi-spheres) labeled as one (1 meant for "good"), and 14 feature-vectors labeled as zero (0, meant for "poor"). The left-over feature-vectors (2 are "good" responders and 4 are "poor" responders) were used as the OOB set (Fig. 1). A PD-subject was classified as a "good" responder if and only if the average predicted as with "good" response and the probability attained for the LH-STN and RH-STN feature-vectors was ≥ 0.5. The predicted UPDRS improvement (%) was computed as the average prediction obtained from the L and R-STN.

2.6 The Performance of Model

In the case of classification, we used the Matthews Cor-relation Coefficient (MCC) for the OOB data as a performance metric, which is a class skew insensitive measure given by

$$MCC = \frac{TP.TN - FP.FN}{(TP + FP)(TP + FN)(TN + FP(TN + FN)}$$

where, TN (TP) and FN (FP) are the numbers of correctly and incorrectly predicted "poor" ("good") response observations, respectively. An MCC value of 1 corresponds to a perfect prediction, while a value of −1 indicates a total

Table 1 Name of features and their corresponding metaphors

Name	Metaphor	Name	Metaphor
$PowerX_W$	Power-band ratio of signal-X in frequency Band-W	RR	Bursting-rate
PKX_W	Peak-to-average power-ratio of signal-X in frequency band-W	PB	Percentage-of-bursts
$FmaxPKX_W$	Frequency corresponding to maximum peak to average power ratio of signal X in frequency band W	FR	Firing-rate
CVX_W	Coefficient of variation of signal X in frequency band W	$stim_E$	coordinates of the stimulation contact on axis E, where E corresponds to x (lateral–medial),y (posteri or–anterior), or z (ventral–dorsal)
$PAFC_{WZ}$	LFP phase–amplitude cross frequency coupling index betwese phase in band **W and voltage in band Z**	stimd	Euclidean-distance of stimulation contact from the STN center
$PPFC_{WZ}$	LFP phase–phase cross frequency coupling index between the phase in band W and amplitude in band Z	dist	Euclidean-distance of STNMER from the stimulation contact
ZeroCrossX	Percentage of electrical-baseline i.e., zero-line crossings in signal X	$distpeak_B$	Distance between the maximum aggregate beta LFP peak and the stimulation contact
SNRX	$20\log_{10}\frac{\sigma X}{\sigma n}, \sigma X = SD(X), \sigma n = \frac{median(X)}{0.7645}$	**hemi**	Hemisphere (Left or Right)
maxCohXY	Maximum coherence between signals X and Y	prep	Preponderance (L/R: most affected body side is the right/left, controlled by the left/right hemisphere)
$maxCohXY_W$	Maximum coherence between signals X and Y in frequency band W	HY	Hoehn and Yahr PD scale
max_PL_W	Maximum phase locking index in band W for the LFP signal	levpre	Preoperative LED
MISI	Mean interspike interval	age	Age
SISI	Interspike interval standard deviation	years	Disease duration
CVISI	Interspike-interval-coefficient-of-variation	sex	sez (female/male coded as 1/2)
PS	Percentage of spikes in the spike signal		

MER-Signals X and Y correspond to LFP, EMUA, or EBUA. The frequency bands W and Z are defined as follows: delta (D; 1–4 Hz), theta (T; 4–10 Hz), beta (B; 10–45 Hz), gamma (G; 45–100 Hz), and high gamma (HG; 100–200 Hz). For example, $maxCohXY_W$ refers to the maximum coherence between LFP and EMUA, LFP and EBUA, or EMUA and EBUA in one of the aforementioned frequency bands

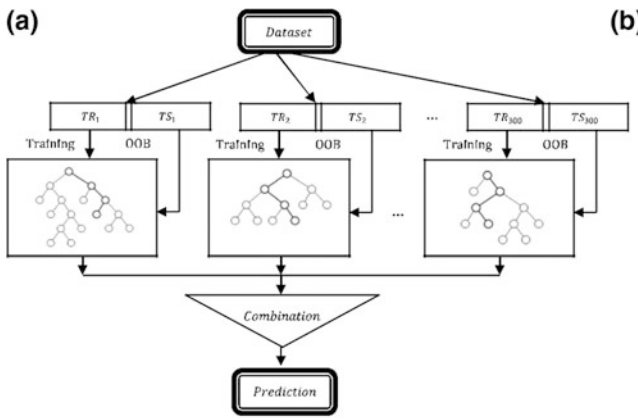

(b)

Random Forest Algorithm	
1	Create 300 decision trees.
2	For each tree the training set consists of 7/9 "good" responders and 7 11 "poor" responders chosen randomly with replacement. The remaining 6 subjects are used as the OOB set.
3	Fit each tree to the training set.
4	Evaluate the performance of each tree on the respective OOB sets.
5	Identify the OOB sets to which a specific subject is included.
6	Extract the respective responses for the left STN and combine them using majority voting for classification or averaging for regression.
7	Repeat step 6 for right STN.
8	Obtain the final prediction by estimating the mean response from the left and right STN.
9	For classification: if the mean response is higher or equal to 0.5, label the patient as a "good" responder; otherwise, label as a "poor" responder. For regression: the predicted UPDRS improvement is the value obtained at step 8.
10	Repeat steps 5-9 for all subjects.
11	Estimate the MCC (classification) or the NMSE (regression) between clinically assessed and predicted responses of all subjects.
12	Assess FI using subject-wise permutation.
13	Remove the feature with the lowest FI.
14	Repeat steps 1-13 until no features are left (Backward elimination selection scheme).
15	Select the combination of features that yield the maximum MCC (classification) or minimum NMSE (regression).

Fig. 1 **a** 300-trees of random forest, in the group, every tree uses a different-training (TR) and testing-set (TS). **b** Sequence of algorithmic steps pursued to foresee for each-subject

disagreement between prediction and observation. Random—classification gives values closure to zero (0). In case of a tie in terms of the MCC value, we chose the classifier that given the minimum cross entropy loss function (J) defined mathematically can be expressed in different ways as follows:

$$J = -\frac{1}{N}\left[\sum_{k=1}^{N} y_k \ln(p_k) + \sum_{k=1}^{N} (1 - y_k)\ln(1 - p_k)\right] \quad (1)$$

$$= -\frac{1}{N}\sum_{k=1}^{N} [y_k \ln(p_k) + \ln(1 - p_k) - y_k \ln(1 - p_k)] \quad (2)$$

$$= -\frac{1}{N}\sum_{k=1}^{N} \{\ln(1 - p_k) + y_k[\ln(p_k) - \ln(1 - p_k)]\} \quad (3)$$

$$= -\frac{1}{N}\sum_{k=1}^{N} \left[\ln(1 - p_k) + yk.\ln\left(\frac{p}{(1 - p_k)}\right)\right] \quad (4)$$

Here, N is total number of patients, y_k is prognostically and/or diagnostically assessed response of subject k, P_k—predicted-response (i.e. average predicted-probability of good response from right and left of subthalamic-nuclei. In connection with the regression—model, the performance is assessed by using the correlation co-efficient (the Pearson's correlation-coefficient, ρ) and the NMSE between the predicted and the clinically assessed UPDRS enhancement (%) output vector for the OOB data. For the classification, Matthews Correlation Coefficient (MCC) is used for the out of bag data as performance-metric as a system of standard measurement [16].

Feature—selections

Feature-significance (FS) is expressed as reduce in the predicted classification or augments in the predicted-regression if the values of this feature is randomly shuffled during the regression phase. This measure was computed for every-tree, averaged and then divided by the following standard deviation (SD) over the whole forest.

$$s^2 = \sqrt{s^2} = \sqrt{\frac{\sum_{i=1}^{n} (x\_\bar{x})^2}{n - 1}} \quad (5)$$

where, $\sigma = \sqrt{\sigma^2}$ is the population (subjects N = 20) standard deviation (SD).

The SD of a sample is square-root-of-variance computed as given in Eq. (5). The combined features given the maximum classification or minimum normalized MSE-regression was chosen.

3 Results

In this study, the STN DBS prediction was considered as a classification—problem. A backward removal feature—selection method and found that four-features attained a maximal MCC-value is 0.9045. Important features found in this study are $PKLFP_{HG}$, power-BUA_T, max-PL_B, and max-PL_{HG} with FIs 0.1495, 0.9142, 0.3899, and 0.5982 correspondingly.

4 Conclusions

UPDR scale is not a rationale but to some extent hypothetical means rationally or scientifically not accepted scale. It is based on clinician's choice scale. Hence for objective—scientific evidence computer simulation and statistical modeling for disease symptoms—or features prediction at early stage be conducted. Then it can be compared with the UPDR scale in terms of the performance improvement after the DBS. Significancy of the work and its importance to the medical physics and biomedical eng: The approach can employ a small number of the signal features inside the STN to predict, separately for each subject, the behavioral outcome of STN DBS, justifying further investigation and, clinical applications possibly. This work has broad implication and innovation of newer statistical and electrophysiological techniques and improving currently available MRI DBS machines for evaluating all types of neurological disorders in particular Parkinson`s disease and other movement disorders. It will be of great interest to the Scientists/engineers involved in medical physics and biomedical research in the fields of biomedical instrumentation and signal processing applications to neuroelectrophysiology.

References

1. Juliann, Schaeffer., New Hope in Neuroprotection? A Parkinson's disease Update. Neuroprotection has become the focus of efforts aimed at slowing the progression of Parkinson`s disease, Nature.-com 1–4 (2017).
2. Benabid, AL., Koudsie, A., Benazzouz, A., Vercueil, L., Fraix V., Chabardes, S., LeBas, JF., Pollak, P.: Deep brain stimulation of the corpus luysi (subthalamic nucleus) and other targets in Parkinson's disease. Extension to new indications such as dystonia and epilepsy. J Neurol 248(3), III37–III47 (2001).
3. Benabid, AL., Krack, PP., Benazzouz, A., Limousin, P., Koudsie, A., Pollak, P.: Deep brain stimulation of the subthalamic nucleus for Parkinson's disease: methodologic aspects and clinical criteria. Neurology 55:S40–S44 (2000).

4. J, Jankovic.: Parkinson's disease: Clinical features and diagnosis. J. Neu-rol. Neurosurg. Psychiatry 79(4), 368–376 (2008).
5. Tugwell, C.: Parkinson's disease in focus. Pharmaceutical Press, London (2008).
6. Yashar, Sarbaz., Hakimeh, Pourakbari.: A review of presented mathematical models in Parkinson's disease: black and gray box models. Med Biol Eng Comput 54, 855–868 (2016).
7. Parkinson, J.: An Essay on Shaking Palsy, Sherwood, Neely and Jones: London (1817).
8. K, Ray Chaudhuri., Victor, SC Fung., Fast Facts: Parkinson`s Disease. Fourth Edition, Health Press Ltd. London (2016).
9. Ronald, F. Pfeiffer., Zbgkiew, K. Wazolek., Manuchair, Ebadi.: Parkinson`s Disease, CRC Press, Taylor & Francis Group (2013).
10. Alim, Luis Benabid.: Laskar Award Winner, Nature Medicine. 10 (20), 1–3 (2014).
11. Mahlon, DeLong.: Laskar Award Winner, Nature Medicine. 10 (20), 4–6 (2014).
12. Larry, Squire., Darwin, Berg., Floyd, E. Bloom., Sascha, du. Lac., Anirvan, Ghosh., Nicholas C. Spitzer.: Fundamental Neuroscience, 4th Edition. *AP* Academic Press (2012).
13. Duane E. Haines., Gregory A. Mihailoff.: Fundamental Neuroscience for Basic and Clinical Applications. E-Book 5th Edition. ELSEVIER (2018).
14. Ashkan, K., Blomstedt, P., Zrinzo, L., Tisch, S., Yousry, T., Limousin-Dowsey, P.: Variability of the subthalamic nucleus: the case for direct MRI guided targeting. Br J Neurosurg. 21 (2), 197–200 (2007).
15. Patel, NK., Khan, S., Gill, SS.: Comparison of atlas- and magnetic-resonance-imaging-based stereotactic targeting of the subthalamic nucleus in the surgical treatment of Parkinson's disease. Stereotact Funct Neurosurg. 86(3), 153–61 (2008).
16. Andrade-Souza, YM., Schwalb, JM., Hamani, C., Eltahawy, H., Hoque, T., Saint-Cyr, J., Lozano, AM.: Comparison of three methods of targeting the subthalamic nucleus for chronic stimulation in Parkinson's disease. Neurosurgery. 62 (2), 875–83 (2008).
17. B. W. Mathews.: Comparison of the predicted and observed secondary structure of T4 phage lysozyme. Biochim. Biophys. Acta. Protein Struct. 405(2), 442–451 (1975).
18. Parkinson J.: An Essay on Shaking Palsy, Sherwood, Neely and Jones: London (1817).